

Short Communication

## Improving the Pitting Corrosion of AISI 434-Based SS Dentistry Drills by Plasma Nitriding

A. E. Muñoz-Castro<sup>1</sup>, R. López-Callejas<sup>1,\*</sup>, R. Valencia-Alvarado<sup>1</sup>, A. Mercado-Cabrera<sup>1</sup>,  
B. G. Rodríguez-Méndez<sup>1</sup>, R. Peña-Eguiluz<sup>1</sup>, A. de la Piedad-Beneítez<sup>2</sup>

<sup>1</sup>Instituto Nacional de Investigaciones Nucleares, Plasma Physics Laboratory, AP 18-1027, 11801 México, D.F.

<sup>2</sup>Instituto Tecnológico de Toluca, AP 890, Toluca, México.

\*E-mail: [regulo.lopez@inin.gob.mx](mailto:regulo.lopez@inin.gob.mx)

Received: 5 February 2015 / Accepted: 15 May 2015 / Published: 28 July 2015

---

The dentistry drills are subjected to fatal failure by pitting corrosion due to both bacterial cleaning and regular use. To prolong the lifetime of these tools a plasma immersion ion implantation (PIII) treatment in a nitrogen atmosphere has been carried out. The as-received drills samples materials consisted of an AISI 434 based stainless steel with 0.6mm diameter and 4mm length. The drills samples were nitrided at -1kV bias with a 20-50  $\mu$ s pulse width and a 200-1000 Hz repetition rate in order to control the temperature between 350°C and 450°C. The X-ray diffraction outcome of the treated drills samples reveals three phases:  $\epsilon$ -Fe<sub>2.3</sub>N, Fe<sub>4.4</sub>N and expanded iron ( $\alpha_N$ ). The micrographs obtained by scanning electron microscopy depict a higher sputtered surface as temperature increases. The pitting corrosion assessed by cyclic potentiodynamic tests showing a good corrosion performance when nitrided at 400°C considering its very narrow hysteresis loop.

---

**Keywords:** Pitting corrosion, plasma immersion ion implantation, ferritic AISI 434, dentistry drills, XRD, SEM.

### 1. INTRODUCTION

Often, tools and mechanical parts are subject to substantial wear, fatigue load and sometimes exposed to corrosive environments, which shorten their lifetime. The process of ion implantation by plasma immersion (PIII) [1-3], is a technique in which a drill sample is placed in a plasma atmosphere and then biased with a negative potential (about 1-100 kV). The latter to direct to the sample ions to increase its solid solubility. PIII has proved a reliable technique for both improving mechanical properties of metals and alloys such as surface hardness, fatigue, wear resistance and electrochemical

performance. However, one of the disadvantages of nitriding results in the white layer ( $\gamma$ -Fe<sub>4</sub>N) formation which can compromise the wear and corrosion resistance [4].

In the area of metal and alloys dental materials, studies cover topics such as wear, hardness, durability, corrosion resistance, antisepsis, disinfection, sterilization, biosafety, etc. The materials used in the dental industry has been evolving, in consequence, it is necessary to create new processes for the treatment of different types of stainless steels as ferritic [5], austenitic [6-10], martensitic [11] and duplex [12]. In particular, the ferritic ones have deserved lesser attention up to now.

The electromechanical response of various stainless steels or alloys has been systematically investigated by corrosion tests and electromechanical measurements [13-16]. Plasma nitriding meets corrosion and wear improvements. And due to its low power consumption, the PIII process is very attractive in processing materials on a large scale. It is not of our knowledge the application of plasma nitriding treatments to improve the fatigue strength of a tiny tool like a dentistry drill.

This work is aimed to enhance the pitting corrosion of dentistry drills made of an AISI 434-based SS due to the chemical cleaning process and the associated fracture failure to prolong their lifetimes. Potentiodynamic tests were used to assess pitting corrosion in treated and untreated samples. X-ray diffraction (XRD) to identify new nitrided phases. Finally, scanning electron microscopy to evaluate elemental nitrogen content and to observe the evolution of the sputtering on the treated sample surfaces.

## 2. EXPERIMENTAL

A DC plasma glow discharge produced by a voltage/current power supply [17] in a nitrogen atmosphere contained in a cylindrical vacuum chamber of SS 316, 0.5 m length, and 0.30 m diameter. The vessel wall has the function of being the cathode of the discharge; while the anode of the discharge consists of an AISI 316 stainless steel rod housed perpendicularly to the chamber axis. DC pulsed power supply achieved the sample bias. The features are -1 kV peak, 20 to 50  $\mu$ s pulse width and 200 to 1000 Hz repetition rate, these with the aim of implementing the temperature control in the drill sample. Prior to making the plasma discharge, using a Balzers vacuum system the chamber pumped down to a  $3 \times 10^{-6}$  mbar base pressure and filled with nitrogen gas up to  $5 \times 10^{-2}$  mbar pressure.

In order to process the commercial drill samples made of AISI 434-based (0.12% C, 1.00% Mn, 1.00% Si, 16-18% Cr, 0.04% P, 0.03% S, 0.75-1.25% Mo and Fe balance) stainless steel of 0.670 mm diameter and 40 mm length. The drill samples placed inside the chamber previously cleaned by an Ar ions bombardment. The nitriding treatments were performed during 4 hours at 350°C, 400°C and 450°C. The drill samples temperature gauged with a type K thermocouple, which clamped to the sample.

The drills analysis was evaluated by different techniques, in our case by scanning electronic microscopy (SEM) operating at 15-25 kV electron energy. The elemental nitrogen content was assessed by EDS analysis associated with SEM under the conditions: 30 kV electron acceleration voltage for untreated sample, and at 25 kV for treated ones; vacuum pressure  $\sim 7.5 \times 10^{-5}$  Torr; acquisition time 150 s and work distance 10 mm. The phases determined by XRD, with a CuK $\alpha$  diffractometer at 35 kV acceleration, 25 mA current CuK $\alpha$   $\lambda=1.5406$  Å, 35°-75° 2 $\theta$ -interval, angular

step 0.01° and step time 3.6 s. The cyclic corrosion test were carried out in a electrochemical cell under the following conditions: 3.5% NaCl aerated solution in distilled water, scanning rate of 1 mV/s, room temperature, three electrodes; one of them is the sample working, other is saturated calomel reference and the platinum auxiliary. The sample ends covered with acrylic.

### 3. RESULTS AND DISCUSSION

#### 3.1. SEM analysis

By EDS determined the nitrogen content in the nitrided working pieces being: 12.2 at% when treated at 350°C, 14 at% and 15.2 at% at 450°C. SEM assessed the nitrogen content and the superficial topographic changes derived from the PIII treatment and whose micrographs labelled considering their particular sample temperatures as: 350 °C (Fig. 1.a), 400 °C (Fig. 1.b) and 450 °C (Fig. 1.c). We can observe in Fig. 1.a a typical microstructure of a stainless steel unveiled by sputtering produced by PIII, the same could say about Fig. 1.b only that, in this case, is more pronounced the sputtering effect. Fig. 1.c shows the most enhanced change of the microstructure due to the combined effect of sputtering and relatively high temperature.

#### 3.2. XRD analysis

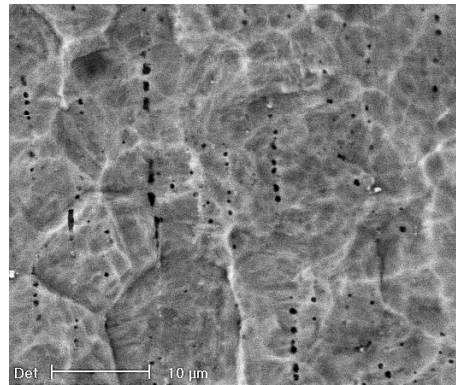
The untreated drill sample displays two XRD peaks corresponding to an  $\alpha$ -iron phase in the (35°-75°)  $2\theta$ -interval (see Fig. 2). These peaks, after nitriding, a left shift is observed showing the presence of an interstitial nitrogen iron expanded phase ( $\alpha_N$ ). Furthermore, other two phases appear: the hexagonal  $\epsilon$ -Fe<sub>2-3</sub>N and the cubic Fe<sub>4.4</sub>N, both the phases and the nitrogen contents depended on temperature.

The relative high nitrogen concentration from the process, the high Cr content of the drills as well as the elevated number of point defects and stresses facilitated the  $\epsilon$ -Fe<sub>2-3</sub>N nucleation [18, 19]. The non-stoichiometric Fe<sub>4.4</sub>N [20, 21] was probably formed by the high number of point defects. The presence of  $\alpha_N$  appears less notorious in the specimen treated at 400°C than 350°C and 450°C ones. This fact could be a consequence of the greatest content of  $\epsilon$ -Fe<sub>2-3</sub>N in the 400°C sample than others (see Fig.2).

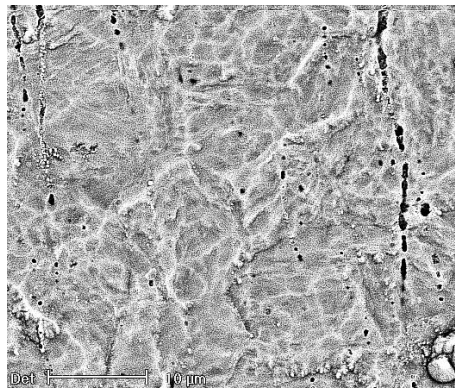
The evolution of  $\epsilon$ -Fe<sub>2-3</sub>N phase with the temperature is achieved at the expense of the  $\alpha$ -iron phase displaying an efficient nitriding in the 450°C sample, at least in the near surface (see Fig. 2). Notice that, in any case, neither precipitation of CrN nor  $\gamma$ -Fe<sub>4</sub>N deleterious phases were present.

#### 3.3. Potentiodynamic Cyclic Tests

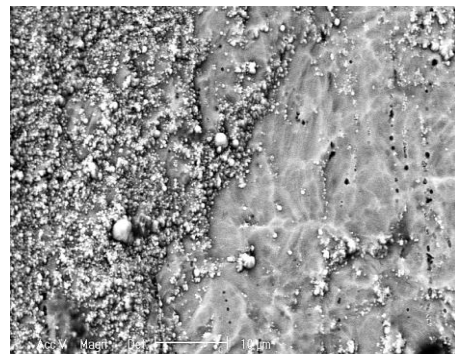
The cycling polarization curve of the as-received sample is showed in Fig. 3.a. This figure shows a clockwise return loop in a descending way as the return sweep potential does in the transpassive region indicating the protective film breakdown and defining the breakdown potential ( $E_b$ ) about 400 mV. The wider hysteresis loop points out a relatively high pitting corrosion susceptibility. Also, the repassivation potential ( $E_{rp}$ ) results lesser than the open circuit potential ( $E_{ocp}$ ) see (Table 1).



(a) 350 °C



(b) 400 °C



(c) 450 °C

**Figure 1.** Micrographs of drills samples treated at indicated different temperatures.

In the drill sample nitrided at 350°C  $E_b$  approaches to 200 mV, and a small right hysteresis return loop is observed in the transpassive region that indicates a slight pitting corrosion susceptibility. As  $E_{ocp} < E_{tp}$  (Table1) a less pitting growth when compared with untreated sample drill. These results can be compared with a nitrided 316 SS by Mirjani *et al.* at 550°, which exhibits a relatively high pitting corrosion [22].

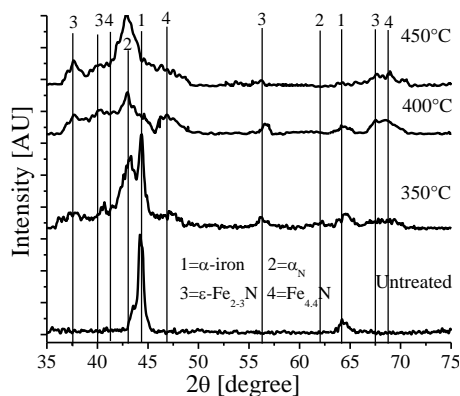


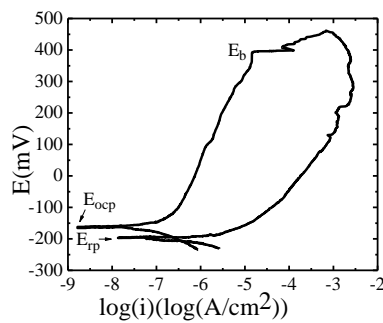
**Figure 2.** X-ray diffractogrammes of the drill samples at different temperatures

Drill samples	$E_b$ [mV]	$E_{ocp}$ [mV]	$E_{rp}$ [mV]
Untreated	400	-180	-200
Treated at 350°C	200	-500	0
Treated at 400°C	-	-450	-350
Treated at 450°C	-	-425	-250

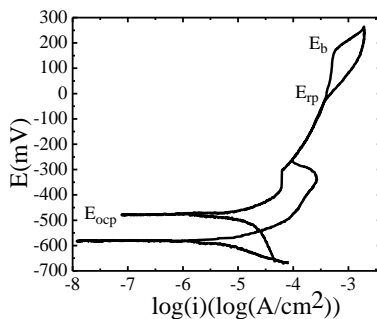
**Table 1.** Potential values of untreated and treated ones of breakdown open circuit and repassivation at different temperatures of the drills.

In the samples treated at 400°C (Fig. 3.c) and 450°C (Fig. 3.d) a very narrow hysteresis loop is observed but is lesser in Fig. 3.c than in Fig. 3.d indicating that both  $E_b$  and the film breakdown do not exist. Nevertheless, current density ( $I$ ) grows one order of magnitude in the potential intervals [-300mV, +100mV] (Fig. 3.c) and [-300mV, +50mV] (Fig. 3.d) then, two pseudo-passive zones are defined. Considering these figures results that the potentials  $E_{ocp} < E_{rp}$  and taking into account that no film breakdown appear the 400°C and 450°C specimens do not almost exhibit pitting corrosion susceptibility. Thus, these samples have a better corrosion performance than 350°C and untreated ones. Contrasting these results with the X10CrNi18-8 samples treated at 1050°C temperature with water cooling [23], ours show a better pitting corrosion resistance.

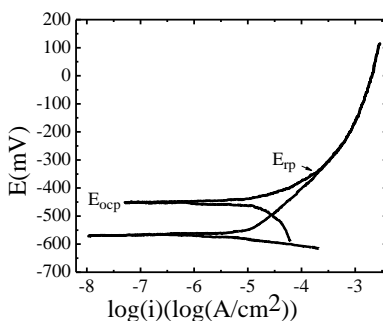
By SEM was obtained that the nitrogen content of the drill sample treated at 450°C was the highest, but the susceptibility to pitting corrosion as good as the treated 400°C (see Figs. 3.c and 3.d). Also, from Fig. 3.b-d, the working temperature range can be defined provided that treatment temperatures do not surpass 450°C. At last, the presence of  $\alpha_N$  does not seem to play a relevant role as seen in Fig. 2 and Fig 3.b-d on the contrary of 316 SS, which is a desired phase [24]. Nevertheless, some loop have found of hysteresis in nitrided steel stainless showing that they are highly prone to pitting but a better performance at general corrosion [22, 23]. But when the pitting corrosion is an issue pulsed PIII nitriding is an excellent option.



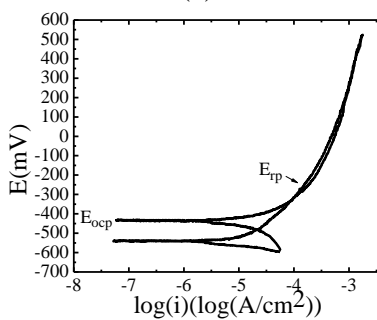
(a)



(b)



(c)



(d)

**Figure 3.** Potentiodynamic polarization curves for the drills: a) untreated, b) 350 °C, c) 400°C, d) 450°C

#### 4. CONCLUSIONS

The PIII nitriding process, to enhance pitting corrosion of a dentistry drill subjected to asepsis, using a DC plasma glow discharge and a pulsed implantation sources, both of low energy consumption. The best performance to pitting corrosion has been obtained in the range 400°C-450°C.

Nevertheless, as the sample temperature reaches around 450°C during the treatment, the enhancement of the pitting corrosion resistance begins to compete with sputtering. Attention must be paid so to avoid both high sputtering and arcing by choosing fair values of voltage, pulse width, and repetition rate. The  $\epsilon$ -Fe<sub>2.3</sub>N and Fe<sub>4.4</sub>N phases improve the pitting corrosion performance. The presence of  $\alpha$ <sub>N</sub> does not play a significant role in pitting corrosion but is not detrimental. Furthermore, the XRD analysis outcome does not suggest the presence of CrN and  $\gamma$ -Fe<sub>4</sub>N, which compromise the corrosion resistance.

#### ACKNOWLEDGEMENTS

This work was partial financial support from CONACYT, Mexico. The authors wish to thank the technical support of María Teresa Torres-Martínez, Pedro Angeles-Espinosa and Isaías Contreras-Villa in the development of the project.

#### References

1. J. R. Conrad, J. L. Radtke, R. A. Dodd, F. J. Worzala, N. C. Tran, *J. Appl. Phys.*, 62-11 (1987) 4591.
2. A.M. Redsten, K. Sridharan, F.J. Worzala, J.R. Conrad, *J. of Mat. Proc. Tech.*, 30-3 (1992) 253.
3. J. Pelletier, A. Anders, *IEEE Trans. on Plasma Sci.*, 33-6 (2005) 1944.
4. André Anders (Editor), *Handbook of Plasma Immersion Ion Implantation*, 1<sup>st</sup> edition, John Wiley & Sons, Inc. New York, 2000.
5. W. Tuckart; M. Gregorio; L. Iurman, *Surf. Eng.*, 26-3 (2010) 185.
6. Y. Li, Z. Wang, L. Wang, *Appl. Surf. Sci.*, 298 (2014) 243.
7. D. Manova, J. Lutz, J.W. Gerlach, H. Neumann, S. Mändl, *Surf. and Coat. Tech.*, 205 (2011) S290.
8. Y.H. Lin, W.C. Lan, K.L. Ou, C.M. Liu, P.W. Peng, *Surf. & Coat. Tech.*, 206-23 (2012) 4785.
9. S. Mändl, R. Dunkel, D. Hirsch, D. Manova, *Surf. & Coat. Tech.*, 258 (2014) 722.
10. T. Shrestha, M. Basirat, I. Charit, G. P. Potirniche, K. K. Rink, U. Sahay, *J Nucl. Mat.* 423 (2012) 110-119.
11. Y. Z. Shen, S. H. Kim, H. D. Cho, Ch. H. Han, W. S. Ryu, *J. of Nucl. Mat.*, 430 (2012) 264.
12. S. Mandl, C. Diaz, J.W. Gerlach, J.A. Garcia, *Nucl. Instrum. and Meth. in Phys. Res. B*, 307 (2013) 305.
13. P. Saravanan, V.S. Raja, S. Mukherjee, *Corros. Sci.*, 74 (2013) 106.
14. Y. Li, S. Zhang, Y. He, L. Zhang, L. Wang, *Mater. and Design*, 64 (2014) 527.
15. L. Shen, L. Wang, Y. Wang, Ch. Wang, *Surf. and Coat. Tech.*, 204 (2010) 3222.
16. P.C. Chen, C.G. Chao and T.F. Liu, *Scripta Materialia* 68 (2013) 380.
17. E. E. Granda-Gutiérrez, R. López-Callejas, R. Peña-Eguiluz, J. S. Benítez-Read, J. O. Pacheco-Sotelo, R. Valencia A., A. Mercado-Cabrera and S. R. Barocio, *Surf. and Coat. Tech.*, 201 (2007) 5454.
18. G. Schreiber, U. Rensch, H. Oettel, C. Blawert, B.L. Mordike, *Surf. and Coat. Tech.*, 169-170 (2003) 447
19. C. Blawert, B.L. Mordike, U. Rensch, G. Schreiber, H. Oettel, *Surf. Engineering* 18-4 (2002) 249
20. F. Mahzoon; M. E. Bahrololoom; S. Javadpour, *Surf. Engineering* 25-8 (2009) 628.
21. H. Nagamatsu, R. Ichiki, Y. Yasumatsu, T. Inoue, M. Yoshida, S. Akamine, S. Kanazawa, *Surf. & Coat. Tech.* 225 (2013) 26.
22. M. Mirjani, J. Mazrooei, N. Karimzadeh, F. Ashrafzadeh, *Surf. and Coat. Tech.*, 206 (2012) 4389.
23. M. Kciuk, A. Kurc-Lisiecka, *Arch. Oat. Sci. and Eng.* 55-2 (2012) 62.

24. C.X. Li, T. Bell, *Corros. Sci.* 46 (2004) 1527

© 2015 The Authors. Published by ESG ([www.electrochemsci.org](http://www.electrochemsci.org)). This article is an open access article distributed under the terms and conditions of the Creative Commons Attribution license (<http://creativecommons.org/licenses/by/4.0/>).